

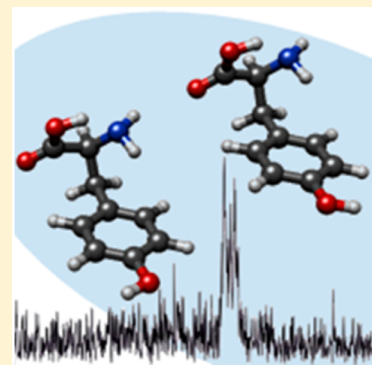
The Rotational Spectrum of Tyrosine

Cristóbal Pérez,[†] Santiago Mata, Carlos Cabezas, Juan C. López, and José. L. Alonso*

Grupo de Espectroscopia Molecular (GEM), Edificio Quifima, Laboratorios de Espectroscopia y Biospectroscopia, Unidad Asociada CSIC, Parque Científico Uva, Universidad de Valladolid, 47011 Valladolid, Spain

S Supporting Information

ABSTRACT: In this work neutral tyrosine has been generated in the gas phase by laser ablation of solid samples, and its most abundant conformers characterized through their rotational spectra. Their identification has been made by comparison between the experimental and *ab initio* values of the rotational and quadrupole coupling constants. Both conformers are stabilized by an O–H•••N hydrogen bond established within the amino acid skeleton chain and an additional weak N–H••• π hydrogen bond. The observed conformers differ in the orientation of the phenolic –OH group.



INTRODUCTION

Proteinogenic amino acids are indispensable agents of biological function since they constitute the building blocks of peptides and proteins. In addition they may have nonprotein functions as neurotransmitters or being precursors of important neurotransmitters or hormones. The function of proteins and their multidimensional structure are highly dependent upon the conformation that their constituent amino acids may adopt. The knowledge of the structure and conformational behavior of those building blocks is thus an important question not only to biochemistry but also for chemistry, since those flexible molecules constitute structural models to study the intermolecular forces that control molecular conformation. The advantage of gas-phase conformational studies lies in the opportunity to obtain the intrinsic properties of the amino acids in isolation, free of the intermolecular interactions which occur in condensed phases where amino acids are bipolar zwitterionic species. Electronic spectroscopy techniques such as high resolution laser-induced fluorescence (LIF) or resonance enhanced multiphoton ionization (REMPI) in combination with supersonic jets have been used to elucidate the structures of gas phase proteogenic amino acids bearing chromophore groups. Hence, these techniques have been applied to tyrosine (Tyr), tryptophan (Trp), and phenylalanine (Phe), which were the subject of a large number of investigations.^{1–18} REMPI and LIF experiments on Tyr^{12–15} reported up to ten vibronic bands which suggested the presence of a large number of stable conformers. More recently, eight different structures of Tyr were confirmed by using UV–UV and IR–UV hole burning techniques.^{16,17} In a last work, using the same experimental approach, Shimozono et al.¹⁸ interpreted the jet cooled electronic spectra on the basis of 12 different conformers.

Microwave spectroscopy is particularly well adapted to the study of multiconformer systems such as amino acids, since it has an inherently high resolution and is exceptionally sensitive to molecular geometry and mass distribution changes and it is not constrained by the need for a chromophore group. However, the vaporization of solid biomolecules imposed serious limitations to study high melting compounds such as amino acids which easily decompose by classical heating methods. Recent developments in laser ablation techniques have allowed us to overcome vaporization problems. In particular, combining Fourier transform microwave spectroscopy with laser ablation techniques in a supersonic expansion (LA-MB-FTMW)^{19–21} has provided a new approach to the structural studies of amino acids. Apart from glycine^{22,23} and alanine,²⁴ first studied by classical heating methods, a large number of proteogenic and nonproteogenic aliphatic amino acids^{19–21,25–34} have been studied by the above technique. Their applicability to aromatic amino acids was first tested in phenylglycine³⁵ and latter applied to the studies of Phe³⁶ and Trp.³⁷ Significant photofragmentation was detected, and consequently, our experimental setup was modified trying to minimize it. Shorter laser pulses (30 ps length pulse) and shorter wavelengths (Nd:YAG 355 nm) have been recently implemented in our new instrumentation^{37,38} in order to minimize photofragmentation processes. In the context of our ongoing investigation of the conformational panorama of amino acids using rotational spectroscopy, we report in this paper the first rotational study of the proteogenic aromatic amino acid tyrosine.

Received: February 24, 2015

Revised: March 31, 2015

Table 1. Experimental Spectroscopic Parameters for the Observed Conformers IIa1 and IIa2 of L-Tyrosine

Parameter ^a	Experimental		Theory	
	Rotamer X	Rotamer Y	Conformer IIa1	Conformer IIa2
A	1529.6791(40) ^b	1525.2543(29)	1519.5	1516.4
B	463.94021(32)	465.48173(25)	472.6	474.2
C	425.76168(40)	427.31023(27)	433.2	434.8
Δ_J	0.0507(29)	0.0527(19)		
χ_{aa}	0.709(14)	0.740(15)	0.94	0.96
χ_{bb}	0.236(88)	0.247(92)	-0.29	-0.28
χ_{cc}	-0.945(88)	-0.988(92)	-0.64	-0.67

^aA, B, and C are the rotational constants; Δ_J is the quartic centrifugal distortion constant; χ_{aa} , χ_{bb} , and χ_{cc} are the diagonal elements of the ¹⁴N nuclear quadrupole coupling tensor. ^bStandard error in parentheses in units of the last digit.

74 ■ EXPERIMENTAL SECTION

75 The rotational spectrum of Tyr was observed using a new laser
76 ablation molecular beam Fourier transform microwave (LA-
77 MB-FTMW)^{20,21,38} spectrometer operating in the 4–10 GHz
78 frequency range. Solid rods of fine-powdered tyrosine (mp
79 290–295 °C) were mixed with minimum quantities of a
80 commercial binder to form a cylindrical rod. The samples were
81 then vaporized using the third harmonic (355 nm) of a
82 Nd:YAG picosecond laser (30 ps length pulse) using energies
83 of ~2 mJ/pulse. The neutral vaporized molecules were seeded
84 in the carrier gas (Ne, 15 bar) and expanded into a Fabry-Pérot
85 resonator. After sending the microwave pulses through the
86 cavity, the emission FID (free induction decay) of the
87 molecules was recorded in the time-domain and Fourier
88 transformed to yield the frequency-domain spectrum. Since the
89 supersonic jet and the microwave resonator axis are collinearly
90 placed, signals appeared split into Doppler doublets. The
91 arithmetic mean of the doublets was taken as the final
92 frequency. The estimated accuracy of the frequency measure-
93 ments is better than 3 kHz.

94 ■ RESULTS AND DISCUSSION

95 Before starting the experimental study, we extended the
96 previous *ab initio* calculations³⁹ on the low energy conformers
97 of Tyr to predict the rotational and nuclear quadrupole
98 coupling constants as well as electric dipole moment
99 components which are needed for the interpretation of the
100 rotational spectrum. Geometry optimizations were carried out
101 with the Gaussian suite of programs⁴⁰ using second-order
102 Møller–Plesset perturbation theory (MP2) in the frozen-core
103 approximation and Pople's 6-311++G(d,p) basis set. This level
104 of theory has proven to give very good results for the rotational
105 parameters at a reasonable computational cost.^{19–33} The
106 calculated spectroscopic parameters for the ten lowest-energy
107 conformers of Tyr are shown in Table S1 of the Supporting
108 Information.

109 All conformers are predicted to be near-prolate asymmetric
110 tops with a nonzero μ_a component of the electric dipole
111 moment. In this way, their R-branch, μ_a -type spectra are
112 expected to show the characteristic patterns consisting of
113 groups of lines separated by approximately $B + C$. Initially, the
114 polarization power was set to optimally polarize the transitions
115 associated with moderate values of μ_a . Hence, we were able to
116 detect two sets of weak μ_a -type R-branch series transitions,
117 attributable to two different rotamers which initially were
118 labeled as X and Y. The subsequent fitting and prediction
119 iterative procedure allows us to observe new μ_a transitions and
120 to extend our measurements to the R-branch μ_b -type spectrum.

All the observed transitions (see Figure S1 and Table S3 and S4
of the Supporting Information) were split into several close
hyperfine components showing the characteristic pattern due to
a ¹⁴N nucleus, which confirms the presence of a single nitrogen
atom in the observed species. This hyperfine structure arises
from the interaction of the electric quadrupole moment of the
¹⁴N ($I = 1$) nucleus with the electric field gradient created at the
site of the quadrupolar nucleus by the rest of the electronic and
nuclear charges of the molecule. This interaction gives rise to
the coupling of the ¹⁴N nuclear spin with the overall angular
momentum, which results in a characteristic hyperfine structure
observable in the rotational spectra. The associated spectro-
scopic parameters are the quadrupole coupling constants $\chi_{\alpha\beta}$
($\alpha\beta = a, b, c$). These are the elements of the quadrupole
coupling tensor χ , which is related to the electric field gradient
tensor q by $\chi = eQq$, where eQ is the electric quadrupole
moment. According to this, the spectra were analyzed⁴¹ using
the semirigid rotor Hamiltonian of Watson in the A reduction
and the I' representation $H_R^{(A)}$,⁴² supplemented with a term to
take into account the quadrupole interaction H_Q ,⁴³ namely $H =$
 $H_R^{(A)} + H_Q$. The analysis allowed the determination of the
rotational constants, the centrifugal distortion constant Δ_J , and
the diagonal elements of the quadrupole coupling tensor for
both X and Y rotamers (see Table 1).

The comparison of the experimental and predicted rotational
parameters in Table 1 shows that the observed rotational
constants are in good agreement with those predicted for
conformers IIa1 and IIa2 (collected also in Table 1 for
comparison). The same conclusion can be reached from the
comparison of the values of the ¹⁴N quadrupole coupling
constants. The experimental values are only in good agreement
with those predicted for conformers IIa1 and IIa2. The values
of the ¹⁴N quadrupole coupling constants are very sensitive to
the orientation of the -NH₂ group with respect to the principal
inertial axis system so that in most cases these constants led to a
conclusive assignment of the observed conformers. However, in
this case, conformers IIa1 and IIa2 have practically the same
values of the ¹⁴N quadrupole coupling constants because the
rotation of the principal inertial axis system induced by the
change in the structure of the phenolic -OH group does not
contribute to significant changes in the quadrupole coupling
constants. Therefore, it is not possible to carry out an
unequivocal assignment of both observed rotamers on the
basis of these constants. Fortunately, the change in orientation
of the -OH group in conformers IIa1 and IIa2 causes
distinctive shifts in the inertial moments which are translated to
the rotational constants. Thus, the small shifts in the rotational
constants do have the key to discern between both conformers.
The changes in the experimental values of the rotational

170 constants between rotamers X and Y are $\Delta A = \Delta A_Y - \Delta A_X \approx$
 171 -4.4 MHz, $\Delta B \approx 1.5$ MHz and $\Delta C \approx 1.5$ MHz. These values
 172 are in good agreement with the differences between the
 173 rotational constants of conformers IIa1 and IIa2; $\Delta A = \Delta A_{IIa2}$
 174 $- \Delta A_{IIa1} \approx -3.1$ MHz, $\Delta B \approx 1.6$ MHz, and $\Delta C \approx 1.6$ MHz.
 175 This fact allows the identification of rotamers X and Y as the
 176 lowest lying energy conformers IIa1 and IIa2, respectively. The
 177 small discrepancy found between the experimental and
 178 predicted values of quadrupole coupling constants (Table 1)
 179 is due to a slight variation in the actual orientation of the amino
 180 group with respect to that predicted via ab initio methods.
 181 Hence, when the amino group rotated (6° on the dihedral
 182 angle $\angle\text{HNCC}$) from the equilibrium value, the predicted and
 183 experimental values of the nuclear quadrupole coupling
 184 constants are nearly in coincidence (see Table S2).

185 In the next stage of our investigation, we focused the
 186 experimental searches to detect spectral signatures of Ia and IIb
 187 conformers, predicted higher in energy. We observed sets of
 188 very weak μ_a -type R-branch rotational transitions in the
 189 predicted frequency intervals for conformers IIb1 and IIb2,
 190 predicted to have high values of the μ_a electric dipole moment
 191 component. We were only able to observe a few lines of each
 192 set with a non-well-resolved hyperfine structure; no spectro-
 193 scopic constants could be derived. After performing wide scans
 194 with different experimental conditions, no lines attributable to
 195 other conformers of Tyr were observed.

196 The two observed conformers of Tyr shown in Figure 1 are
 197 stabilized by an O–H \cdots N hydrogen bond with a COOH trans

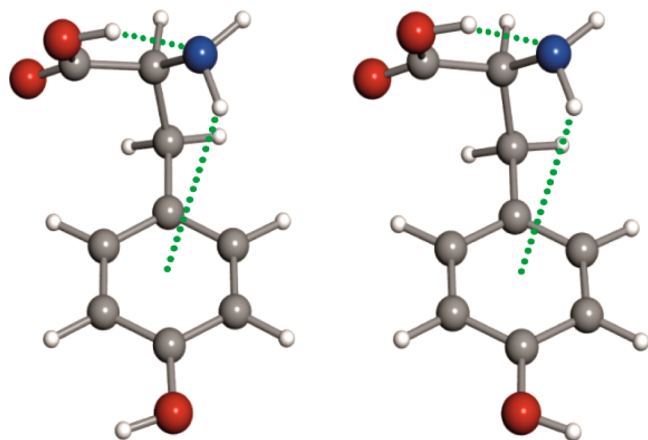


Figure 1. 3D structures of observed conformers (IIa1(left) and IIa2 (right)) of Tyr showing the intramolecular interactions which stabilize both structures.

198 configuration (type II of the amino acids²⁰). Moreover, one of
 199 the hydrogen atoms of the amino group is pointing toward the
 200 π electron density of the ring, indicating the existence of an N–
 201 H $\cdots\pi$ interaction. The modified orientation of the amino group
 202 mentioned above points to the establishment of this N–H $\cdots\pi$
 203 interaction by decreasing the hydrogen bond distance. Both
 204 intramolecular hydrogen bonds form a chain that reinforces
 205 their strength through cooperative effects.^{44,45} For the over-
 206 whelming majority of the α -amino acids studied so far, a type I
 207 conformer has been found as global minimum. A few
 208 exceptions have been found for which a type II conformer
 209 has been found to be the most stable conformer. Those include
 210 the imino acids proline,^{19,32} and hydroxyproline,²⁸ asparagine,³⁴
 211 phenylalanine,³⁶ tryptophan,³⁷ and histidine.³⁸ With the

exception of proline and hydroxyproline, the type II O–H \cdots 212
 N hydrogen bond established within the amino acid backbone 213
 is reinforced by an additional bond from the amino group to 214
 the lateral chain in all cases. In the case of the phenylalanine,³⁶ 215
 tryptophan,³⁷ and tyrosine, this additional interaction corre- 216
 sponds to a weak N–H $\cdots\pi$ weak hydrogen bond. 217

Relative intensity measurements on selected μ_a -type lines of 218
 the IIa1 and IIa2 conformers indicate that the relative 219
 populations follow the order IIa2 > IIa1, in agreement with 220
 the theoretically predicted relative energies. This pair of 221
 conformers, which differ only in the OH arrangement, have a 222
 predicted energy difference of 132 cm^{-1} . This energy difference 223
 could be tentatively explained by the existence of local dipole– 224
 local dipole⁴⁶ interaction between the amino acid group and the 225
 side chain ($-\text{CH}_2-\text{C}_6\text{H}_4-\text{OH}$). These dipoles find a more 226
 favorable arrangement for conformer IIa2, increasing in this 227
 way the relative stability of this conformer. 228

In conclusion, we have observed two conformers of Tyr 229
 through the analysis of its rotational spectrum. These 230
 conformers are stabilized by O–H \cdots N and N–H $\cdots\pi$ hydrogen 231
 bond interactions and derive from the most stable forms 232
 observed for the related amino acid Phe.³⁶ The weakness of the 233
 spectrum and the low number of observed conformers for Tyr 234
 compared with those detected for aliphatic amino acids^{30–33} 235
 can be attributable to photofragmentation/ionization processes 236
 during the laser ablation course. As reported for Phe,⁴⁷ 237
 ionization processes would favor the presence of only IIa and 238
 IIb conformers, with higher ionization energy, in the supersonic 239
 jet. We have monitored photofragmentation effects using a 240
 time-of-flight mass spectrometer (TOF-MS) coupled with the 241
 same laser ablation nozzle used in our LA-MB-FTMW 242
 experiment and we found (See Figure S2 of the Supporting 243
 Information) a large amount of Tyr fragments, indicating that 244
 photofragmentation of Tyr occurs to a large extent in the 245
 ablation process. The subsequent depletion of the number 246
 density of tyrosine in the supersonic expansion would cause the 247
 observation of weaker spectra. Despite the important improve- 248
 ments recently achieved in the observation of nucleoside 249
 uridine,⁴⁸ the intrinsic effects of photofragmentation associated 250
 with the aromatic amino acids make extremely difficult the 251
 observation of their complete conformational panorama. 252

■ ASSOCIATED CONTENT

📄 Supporting Information

Complete ref 40, predicted ab initio molecular properties for 255
 the lower-energy conformers of the tyrosine together with 256
 MP2/6-311++G(d,p) equilibrium principal axis coordinates, 257
 quadrupole coupling constants calculated at the different 258
 dihedral angles $\angle\text{HNCC}$ for the observed conformers, 259
 observed rotational transitions for the two detected conformers, 260
 and list of measured transitions and mass spectrum of tyrosine. 261
 This material is available free of charge via the Internet at 262
<http://pubs.acs.org>. 263

■ AUTHOR INFORMATION

Corresponding Author

* E-mail: jalonso@qf.uva.es Phone: +34 983186348 Fax: +34 266
 983186349. 267

Present Address

†(C.P.) Max-Planck Institute for the Structure and Dynamics of 269
 Matter; Luruper Chaussee 149, D-22761 Hamburg. Germany. 270

271 **Notes**

272 The authors declare no competing financial interest.

273 ■ **ACKNOWLEDGMENTS**

274 This research was supported by Ministerio de Ciencia e
275 Innovación (grant numbers CTQ 2010-19008, CTQ 2013-
276 40717-P, and Consolider Ingenio 2010 CSD 2009-00038) and
277 Junta de Castilla y León (grant number VA175U13). C.C.
278 thanks the Junta de Castilla y León for the postdoctoral
279 contract (grant number CIP13/01).

280 ■ **REFERENCES**

281 (1) Philips, L. A.; Webb, S. P.; Martinez, S. J.; Fleming, G. R.; Levy,
282 D. H. Time-Resolved Spectroscopy of Tryptophan Conformers in a
283 Supersonic Jet. *J. Am. Chem. Soc.* **1988**, *110*, 1352–1355.
284 (2) Rizzo, T. R.; Park, Y. D.; Peteanu, L. A.; Levy, D. H. The
285 Electronic Spectrum of the Amino Acid Tryptophan in the Gas Phase.
286 *J. Chem. Phys.* **1986**, *84*, 2534–2541.
287 (3) Cable, J. R.; Tubergen, M. J.; Levy, D. H. Laser Desorption
288 Molecular Beam Spectroscopy: The Electronic Spectra of Tryptophan
289 Peptides in the Gas Phase. *J. Am. Chem. Soc.* **1987**, *109*, 6198–6199.
290 (4) Snoek, L. C.; Kroemer, R. T.; Hockridge, M. R.; Simons, J. P.
291 Conformational Landscapes of Aromatic Amino Acids in the Gas
292 Phase: Infrared and Ultraviolet Ion Dip Spectroscopy of Tryptophan.
293 *Phys. Chem. Chem. Phys.* **2001**, *3*, 1819–1826.
294 (5) Snoek, L. C.; Kroemer, R. T.; Simons, J. P. A Spectroscopic and
295 Computational Exploration of Tryptophan–Water Cluster Structures
296 in the Gas Phase. *Phys. Chem. Chem. Phys.* **2002**, *4*, 2130–2139.
297 (6) Martinez, S. J., III; Alfano, J. C.; Levy, D. H. The Electronic
298 Spectroscopy of Tyrosine and Phenylalanine Analogs in a Supersonic
299 Jet: Acidic Analogs. *J. Mol. Spectrosc.* **1991**, *145*, 100–111.
300 (7) Snoek, L. C.; Robertson, E. G.; Kroemer, R. T.; Simons, J. P.
301 Conformational Landscapes in Amino Acids: Infrared and Ultraviolet
302 Ion-Dip Spectroscopy of Phenylalanine in the Gas Phase. *Chem. Phys.*
303 *Lett.* **2000**, *321*, 49–56.
304 (8) Lee, K. T.; Sung, J.; Lee, K. J.; Kim, S. K.; Park, Y. D. Resonant
305 Two-Photon Ionization Study of Jet-Cooled Amino Acid: L-Phenyl-
306 alanine and Its Monohydrated Complex. *J. Chem. Phys.* **2002**, *116*,
307 8251–8254.
308 (9) Lee, K. T.; Sung, J.; Lee, K. J.; Park, Y. D.; Kim, S. K.
309 Conformation-Dependent Ionization Energies of L-Phenylalanine.
310 *Angew. Chem., Int. Ed.* **2002**, *41*, 4114–4117.
311 (10) Hashimoto, T.; Takasu, Y.; Yamada, Y.; Ebata, T. Anomalous
312 Conformer Dependent S1 Lifetime of L-Phenylalanine. *Chem. Phys.*
313 *Lett.* **2006**, *421*, 227–231.
314 (11) Ebata, T.; Hashimoto, T.; Ito, T.; Inokuchi, Y.; Altunsoy, F.;
315 Brutschy, B.; Tarakeshwar, P. Hydration Profiles of Aromatic Amino
316 Acids: Conformations and Vibrations of L-phenylalanine–(H₂O)_n
317 Clusters. *Phys. Chem. Chem. Phys.* **2006**, *8*, 4783–4791.
318 (12) Martinez, S. J., III; Alfano, J. C.; Levy, D. H. The Electronic
319 Spectroscopy of the Amino Acids Tyrosine and Phenylalanine in a
320 Supersonic Jet. *J. Mol. Spectrosc.* **1992**, *156*, 421–430.
321 (13) Martinez, S. J.; Alfano, J. C.; Levy, D. H. The Electronic
322 Spectroscopy of Tyrosine and Phenylalanine Analogs in a Supersonic
323 Jet: Basic Analogs. *J. Mol. Spectrosc.* **1993**, *158*, 82–92.
324 (14) Lindinger, A.; Toennies, J. P.; Vilesov, A. F. High Resolution
325 Vibronic Spectra of the Amino Acids Tryptophan and Tyrosine in 0.38
326 K Cold Helium Droplets. *J. Chem. Phys.* **1999**, *110*, 1429–1436.
327 (15) Grace, L. I.; Cohen, R.; Dunn, T. M.; Lubman, D. M.; de Vries,
328 M. S. The R2PI Spectroscopy of Tyrosine: A Vibronic Analysis. *J. Mol.*
329 *Spectrosc.* **2002**, *215*, 204–219.
330 (16) Inokuchi, Y.; Kobayashi, Y.; Ito, T.; Ebata, T. Conformation of
331 L-Tyrosine Studied by Fluorescence-Detected UV–UV and IR–UV
332 Double-Resonance Spectroscopy. *J. Phys. Chem. A* **2007**, *111*, 3209–
333 3215.
334 (17) Abo-Riziq, A.; Grace, L.; Crews, B.; Callahan, M. P.; van
335 Mourik, T.; de Vries, M. S. Conformational Structure of Tyrosine,

Tyrosyl-glycine, and Tyrosyl-glycyl-glycine by Double Resonance
Spectroscopy. *J. Phys. Chem. A* **2011**, *115*, 6077–6087. 336
(18) Shimozono, Y.; Yamada, K.; Ishiuchi, S.; Tsukiyama, K.; Fujii,
337 M. Revised Conformational Assignments and Conformational
338 Evolution of Tyrosine by Laser Desorption Supersonic Jet Laser
339 Spectroscopy. *Phys. Chem. Chem. Phys.* **2013**, *15*, 5163–5175. 341
(19) Lesarri, A.; Mata, S.; Cocinero, E. J.; Blanco, S.; López, J. C.;
342 Alonso, J. L. The Structure of Neutral Proline. *Angew. Chem., Int. Ed.*
343 **2002**, *41*, 4673–4676.
(20) Alonso, J. L.; Pérez, C.; Sanz, M. E.; López, J. C.; Blanco, S.
344 Seven Conformers of L-Threonine in the Gas Phase: A LA-MB-
345 FTMW Study. *Phys. Chem. Chem. Phys.* **2009**, *11*, 617–627. 347
(21) Peña, I.; Sanz, M. E.; López, J. C.; Alonso, J. L. Preferred
348 Conformers of Proteinogenic Glutamic Acid. *J. Am. Chem. Soc.* **2011**,
349 *134*, 2305–2312. 350
(22) Brown, R. D.; Godfrey, P. D.; Storey, J. W. V.; Bassez, M.-P.
351 Microwave Spectrum and Conformation of Glycine. *J. Chem. Soc.,*
352 *Chem. Commun.* **1978**, 547–548. 353
(23) Suenram, R. D.; Lovas, F. J. Millimeter Wave Spectrum of
354 Glycine. *J. Mol. Spectrosc.* **1978**, *72*, 372–382. 355
(24) Godfrey, P. D.; Firth, S.; Hatherley, L. D.; Brown, R. D.; Pierlot,
356 A. P. Millimeter-Wave Spectroscopy of Biomolecules: Alanine. *J. Am.*
357 *Chem. Soc.* **1993**, *115*, 9687–9691. 358
(25) Blanco, S.; Lesarri, A.; López, J. C.; Alonso, J. L. The Gas-Phase
359 Structure of Alanine. *J. Am. Chem. Soc.* **2004**, *126*, 11675–11683. 360
(26) Lesarri, A.; Cocinero, E. J.; López, J. C.; Alonso, J. L. The Shape
361 of Neutral Valine. *Angew. Chem., Int. Ed.* **2004**, *43*, 605–610. 362
(27) Lesarri, A.; Sánchez, R.; Cocinero, E. J.; López, J. C.; Alonso, J.
363 L. Coded Amino Acids in Gas Phase: The Shape of Isoleucine. *J. Am.*
364 *Chem. Soc.* **2005**, *127*, 12952–12956. 365
(28) Lesarri, A.; Cocinero, E. J.; López, J. C.; Alonso, J. L. Shape of
366 4(S)- and 4(R)-Hydroxyproline in Gas Phase. *J. Am. Chem. Soc.* **2005**,
367 *127*, 2572–2579. 368
(29) Cocinero, E. J.; Lesarri, A.; Grabow, J.-U.; López, J. C.; Alonso,
369 J. L. The Shape of Leucine in the Gas Phase. *ChemPhysChem* **2007**, *8*,
370 599–604. 371
(30) Blanco, S.; Sanz, M. E.; López, J. C.; Alonso, J. L. Revealing the
372 Multiple Structures of Serine. *Proc. Natl. Acad. Sci.* **2007**, *104*, 20183–
373 20188. 374
(31) Sanz, M. E.; Blanco, S.; López, J. C.; Alonso, J. L. Rotational
375 Probes of Six Conformers of Neutral Cysteine. *Angew. Chem., Int. Ed.*
376 **2008**, *47*, 6216–6220. 377
(32) Mata, S.; Vaquero, V.; Cabezas, C.; Peña, I.; Pérez, C.; López, J.
378 C.; Alonso, J. L. Observation of Two New Conformers of Neutral
379 Proline. *Phys. Chem. Chem. Phys.* **2009**, *11*, 4141–4144. 380
(33) Sanz, M. E.; López, J. C.; Alonso, J. L. Six Conformers of
381 Neutral Aspartic Acid Identified in the Gas Phase. *Phys. Chem. Chem.*
382 *Phys.* **2010**, *12*, 3573–3578. 383
(34) Cabezas, C.; Varela, M.; Peña, I.; Mata, S.; López, J. C.; Alonso,
384 J. L. The Conformational Locking of Asparagine. *Chem. Commun.*
385 **2012**, 48, 5934–5936. 386
(35) Sanz, M. E.; Cortijo, V.; Caminati, W.; López, J. C.; Alonso, J. L.
387 The Conformers of Phenylglycine. *Chem.—Eur. J.* **2006**, *12*, 2564–
388 2570. 389
(36) Pérez, C.; Mata, S.; Blanco, S.; López, J. C.; Alonso, J. L. Jet-
390 Cooled Rotational Spectrum of Laser-Ablated Phenylalanine. *J. Phys.*
391 *Chem. A* **2011**, *115*, 9653–9657. 392
(37) Sanz, M. E.; Cabezas, C.; Mata, S.; Alonso, J. L. Rotational
393 Spectrum of Tryptophan. *J. Chem. Phys.* **2014**, *140*, 204308. 394
(38) Bermúdez, C.; Mata, S.; Cabezas, C.; Alonso, J. L. Tautomerism
395 in Neutral Histidine. *Angew. Chem., Int. Ed.* **2014**, *53*, 11015–11018. 396
(39) Zhang, M.; Huang, Z.; Lin, Z. Systematic Ab Initio Studies of
397 the Conformers and Conformational Distribution of Gas-Phase
398 Tyrosine. *J. Chem. Phys.* **2005**, *122*, 134313. 399
(40) Frisch, M. J.; Trucks, G. W.; Schlegel, H. B.; Scuseria, G. E.;
400 Robb, M. A.; Cheeseman, J. R.; Montgomery, J. A., Jr.; Vreven, T.;
401 Kudin, K. N.; Burant, J. C.; et al. GAUSSIAN 03 (Revision B.04) (See
402 Supporting Information for full citation). 403

- 404 (41) Pickett, H. M. The Fitting and Prediction of Vibration-Rotation
405 Spectra with Spin Interactions. *J. Mol. Spectrosc.* **1991**, *148*, 371–377.
- 406 (42) Watson, J. K. G. In *Vibrational Spectra and Structure*; Durig, J. R.,
407 Ed.; Elsevier: New York, 1977; Vol. 6, pp 1– 78.
- 408 (43) Gordy, W.; Cook, R. L. *Microwave Molecular Spectra*, 3rd ed.;
409 Wiley: New York, 1984.
- 410 (44) Saenger, W. *Nature (London)* **1979**, *279*, 343.
- 411 (45) Jeffrey, G. A. *An Introduction to Hydrogen Bonding*; Oxford
412 University Press: New York, 1997.
- 413 (46) *The Weak Hydrogen Bond in Structural Chemistry and Biology*;
414 IUCr Monographs on Crystallography, Vol. IX; Desiraju, G. R.,
415 Steiner, T., Eds.; Oxford University Press: Oxford, 2001.
- 416 (47) Lee, K. T.; Sung, J.; Lee, K. J.; Park, Y. D.; Kim, S. K.
417 Conformation-dependent ionization energies of L-phenylalanine.
418 *Angew Chem., Int. Ed.* **2002**, *41*, 4114–4117.
- 419 (48) Peña, I.; Cabezas, C.; Alonso, J. L. The Nucleoside Uridine
420 Isolated in the Gas Phase. *Angew. Chem., Int. Ed.* **2015**, *10*, 2991–2994.